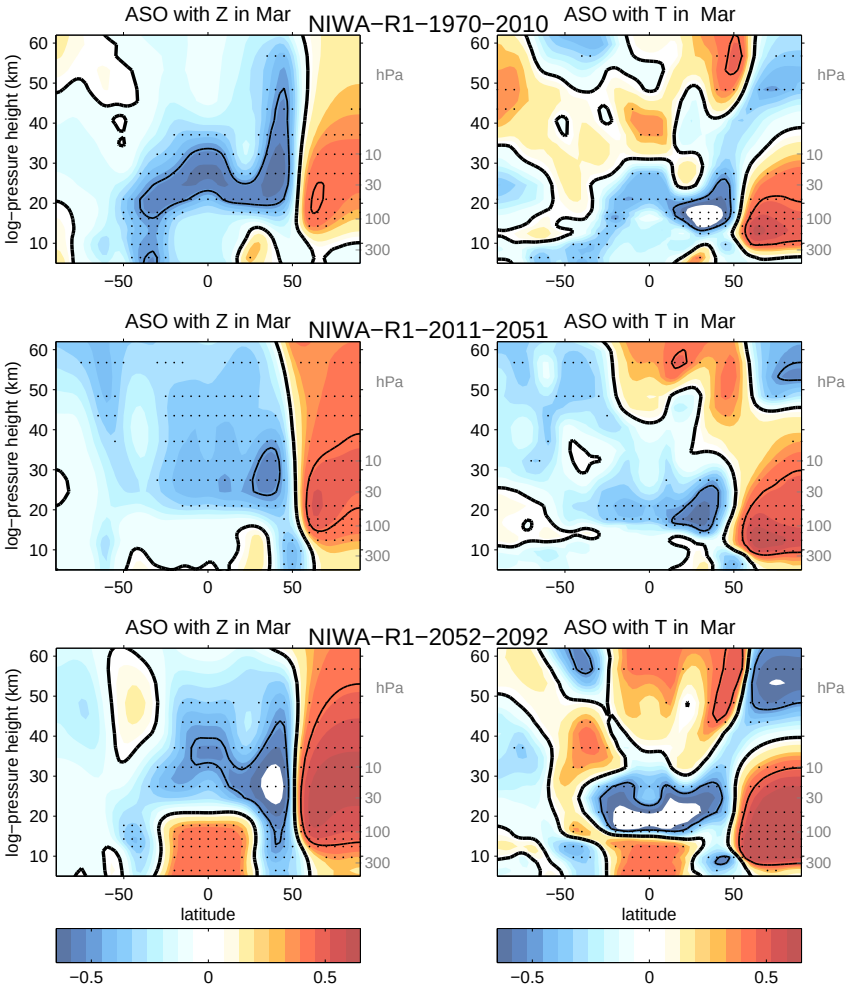

Fig. S 1. As in figure 2 of main body, but for Niwa run #1

1 Influence of Arctic Stratospheric Ozone on Surface Climate in CCMI models

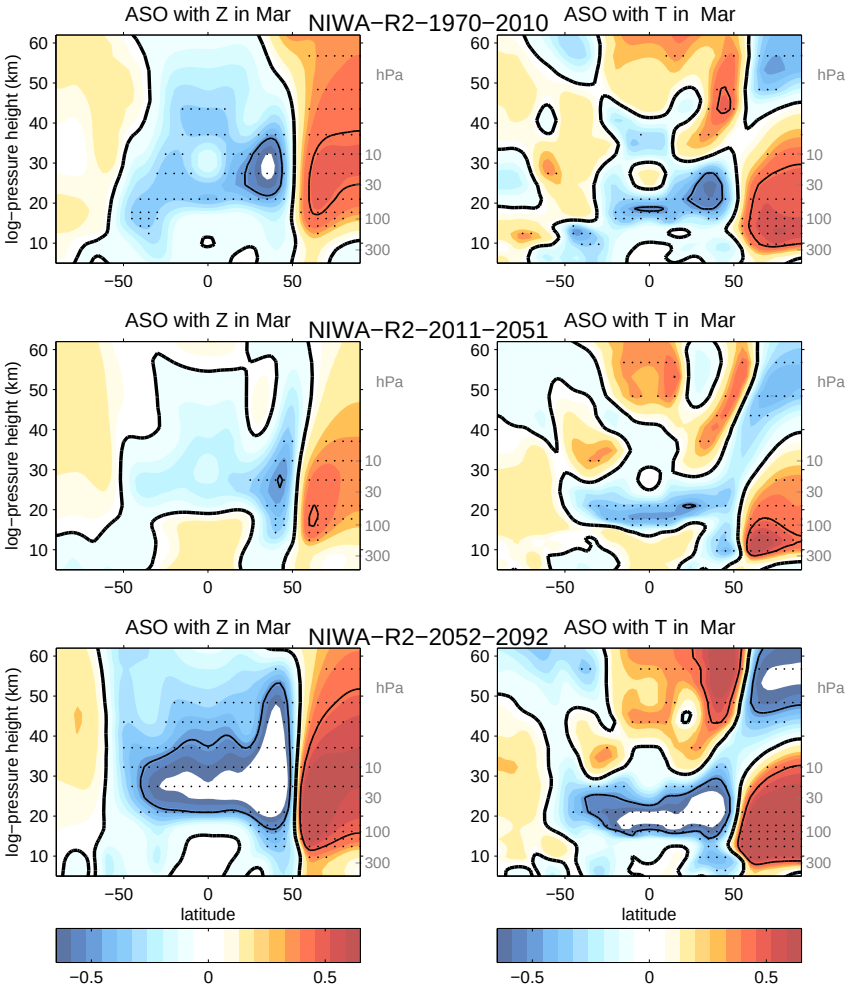

Fig. S 2. As in figure 2 of main body, but for Niwa run #2

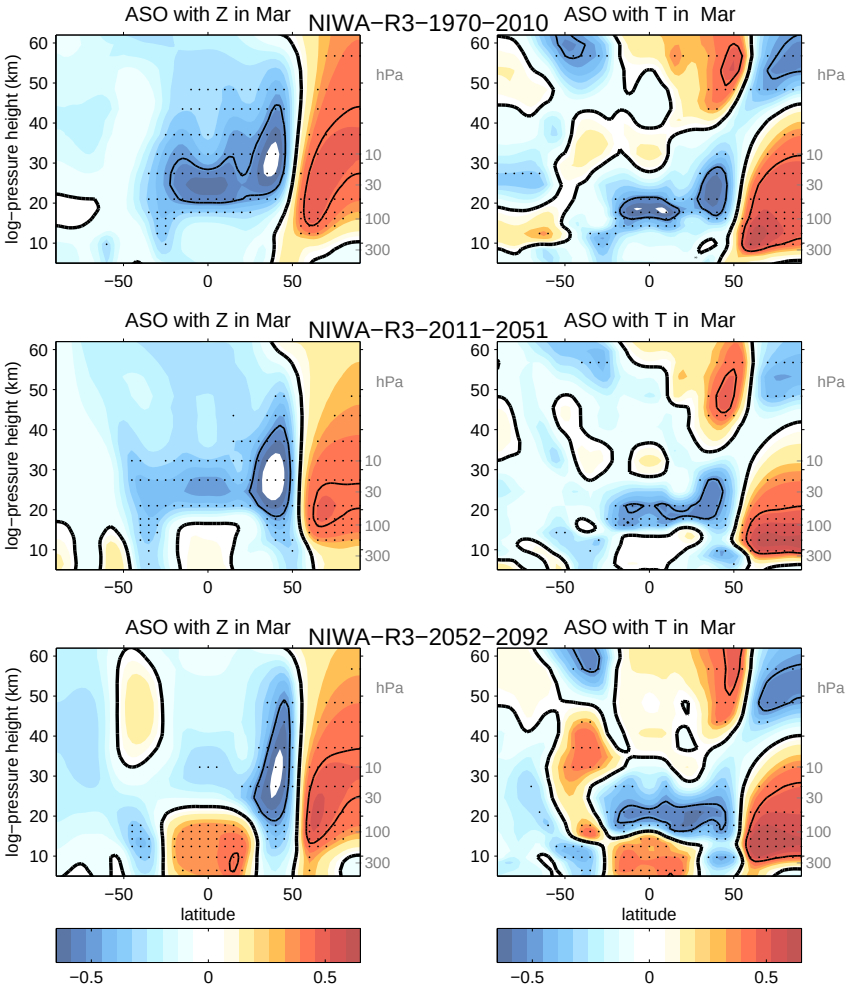

Fig. S 3. As in figure 2 of main body, but for Niwa run #3

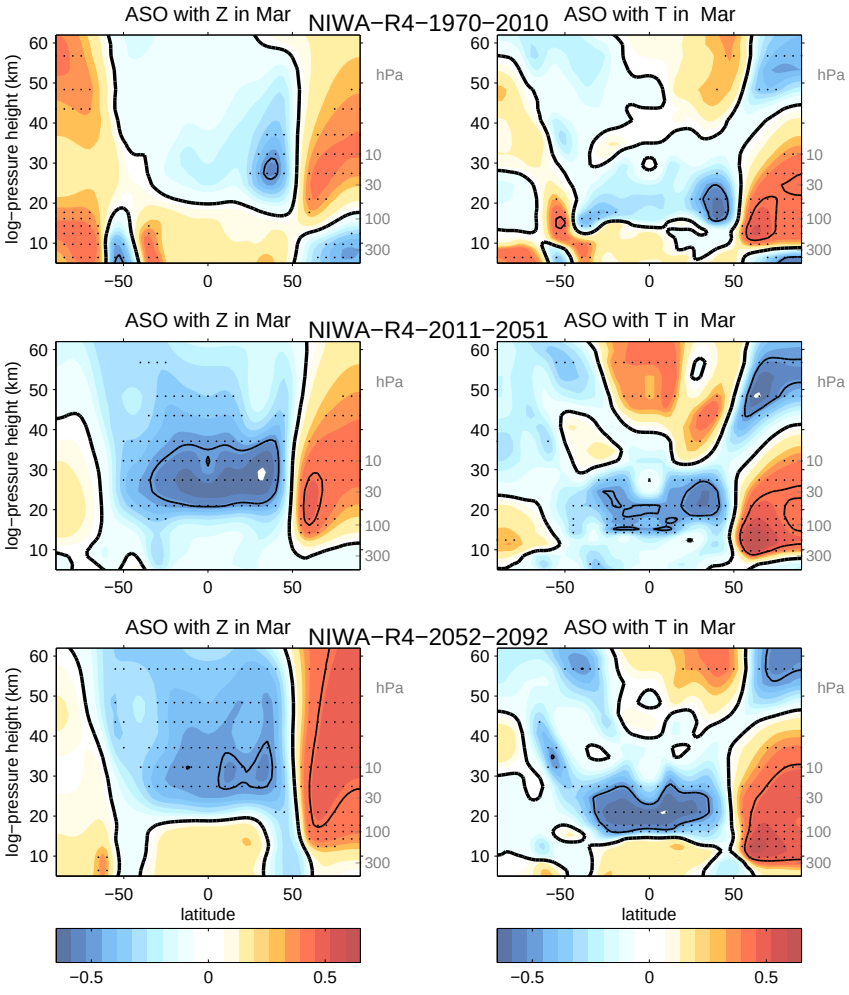

Fig. S 4. As in figure 2 of main body, but for Niwa run #4

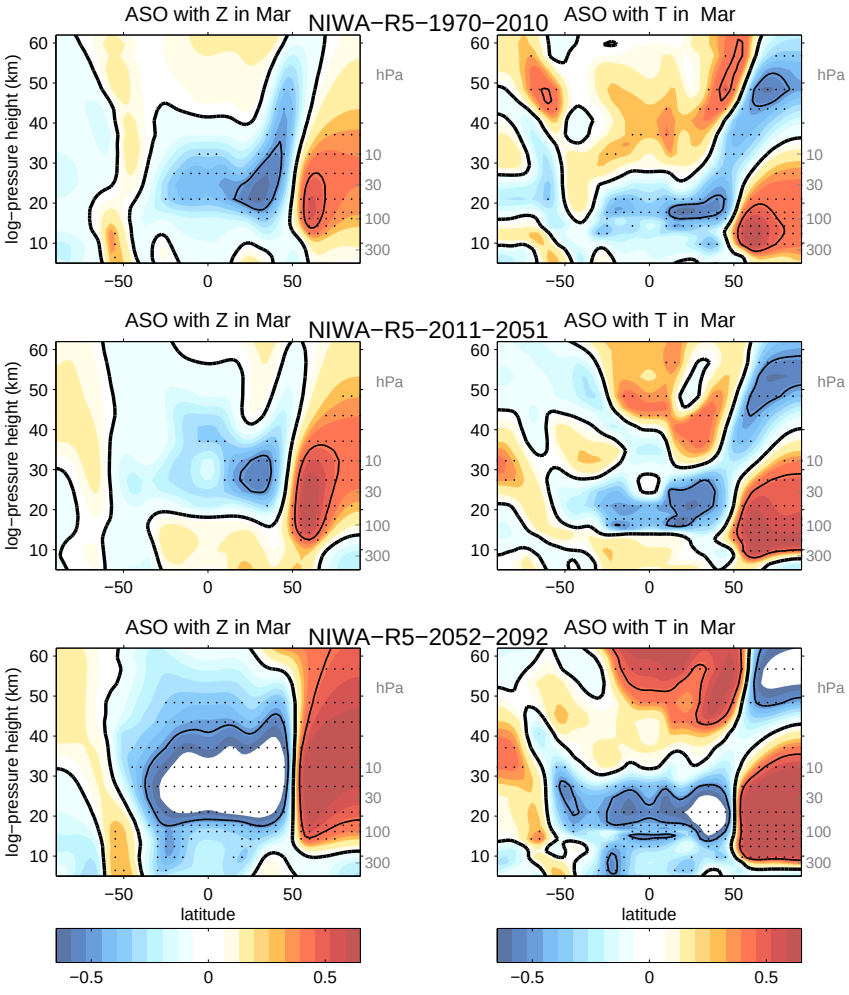

Fig. S 5. As in figure 2 of main body, but for Niwa run #5

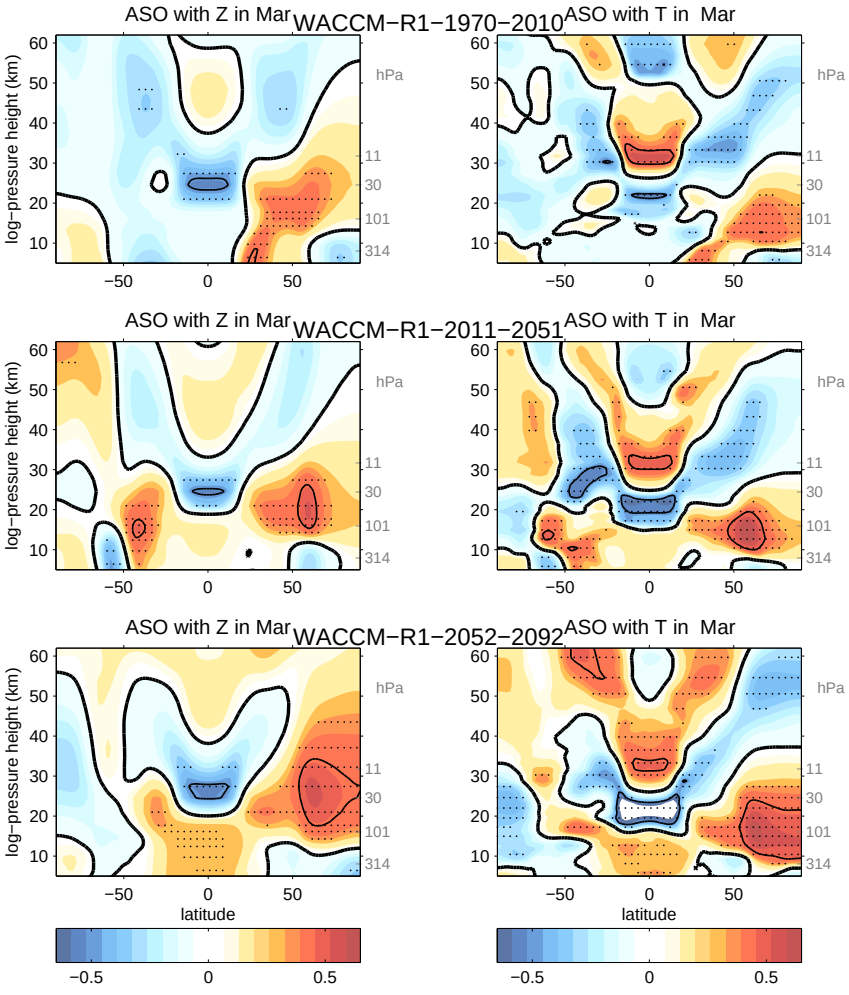

Fig. S 6. As in figure 2 of main body, but for NCAR-WACCM run #1

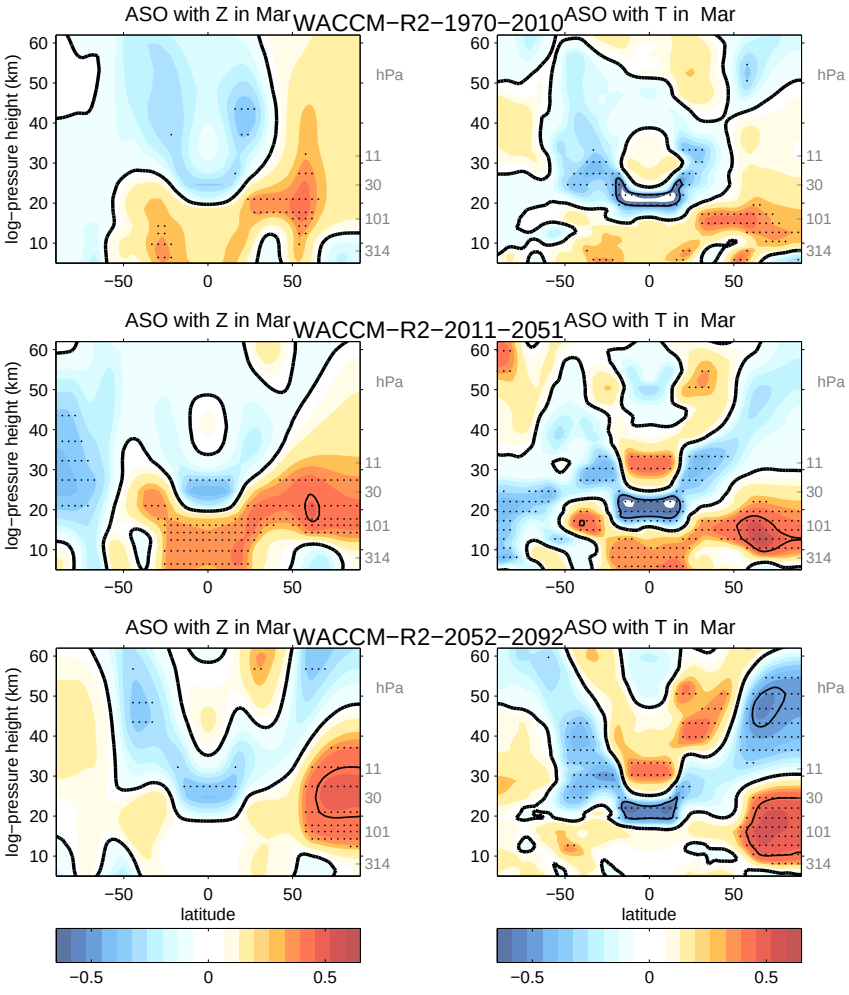

Fig. S 7. As in figure 2 of main body, but for NCAR-WACCM run #2

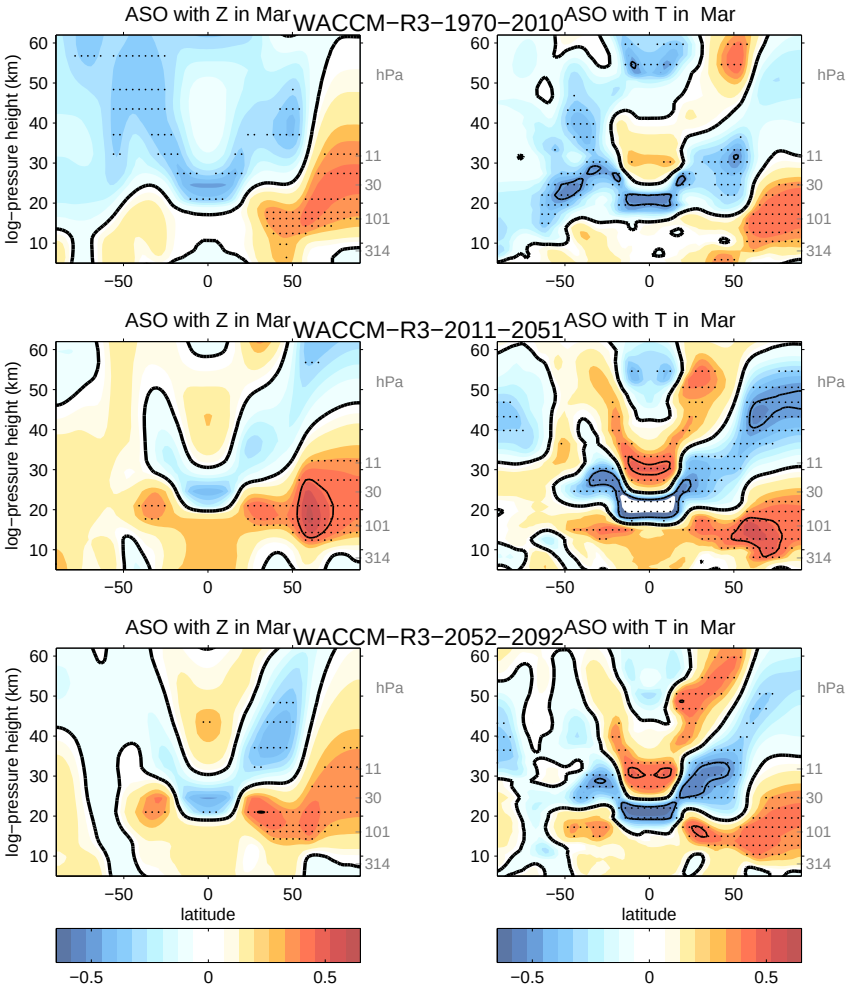

Fig. S 8. As in figure 2 of main body, but for NCAR-WACCM run #3

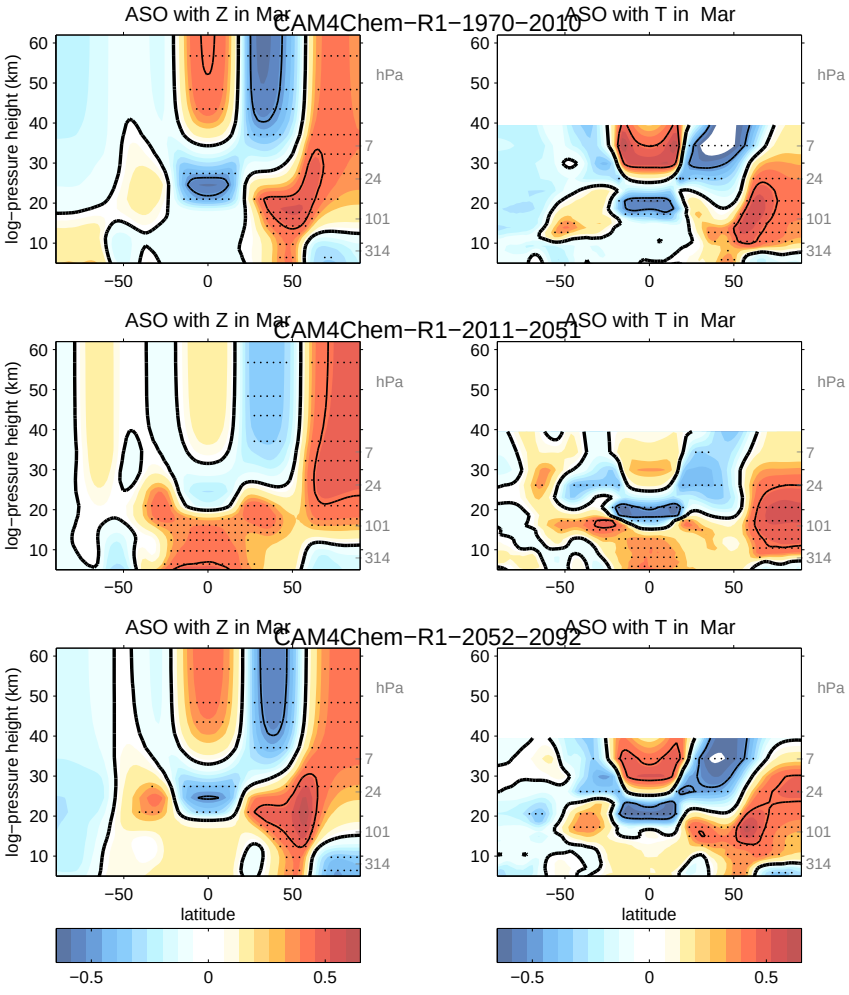

Fig. S 9. As in figure 2 of main body, but for NCAR-CAM4Chem run #1

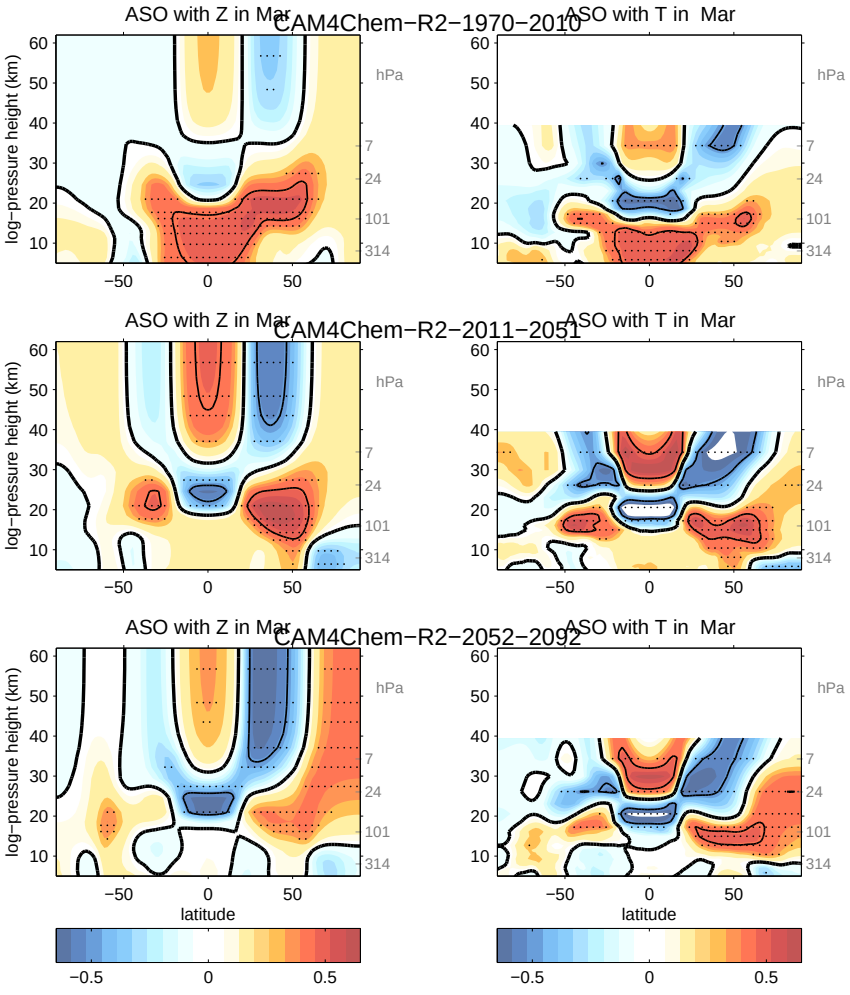

Fig. S 10. As in figure 2 of main body, but for NCAR-CAM4Chem run #2

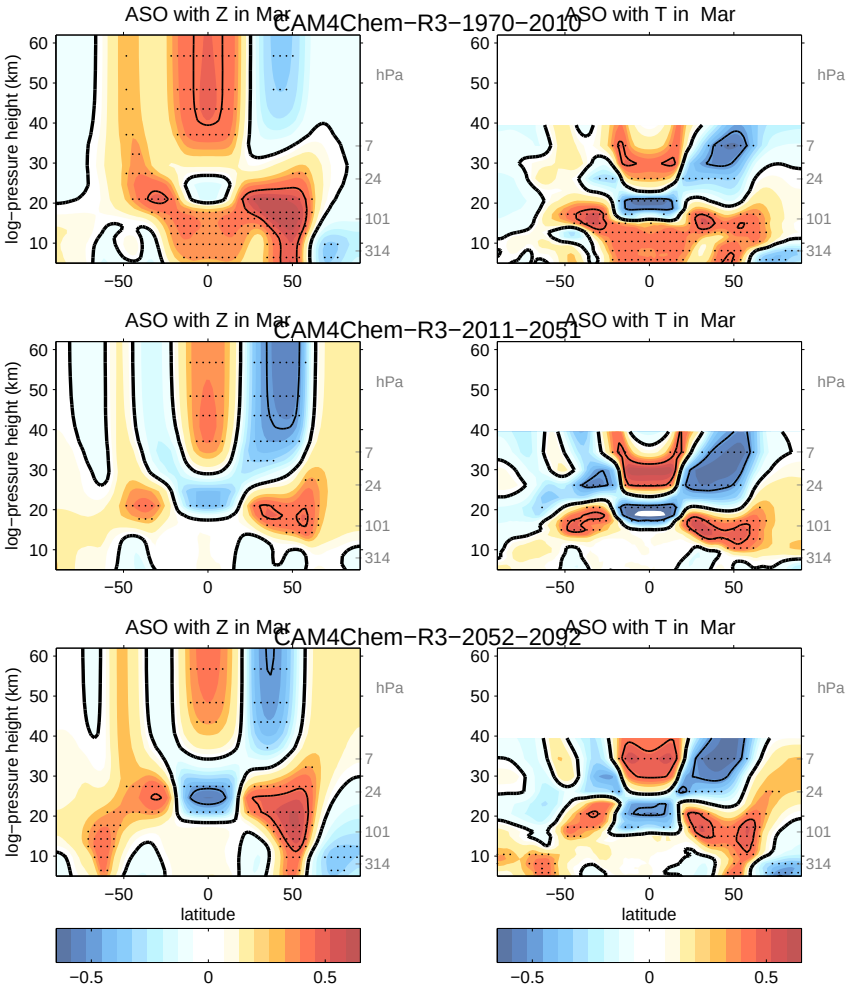

Fig. S 11. As in figure 2 of main body, but for NCAR-CAM4Chem run #3

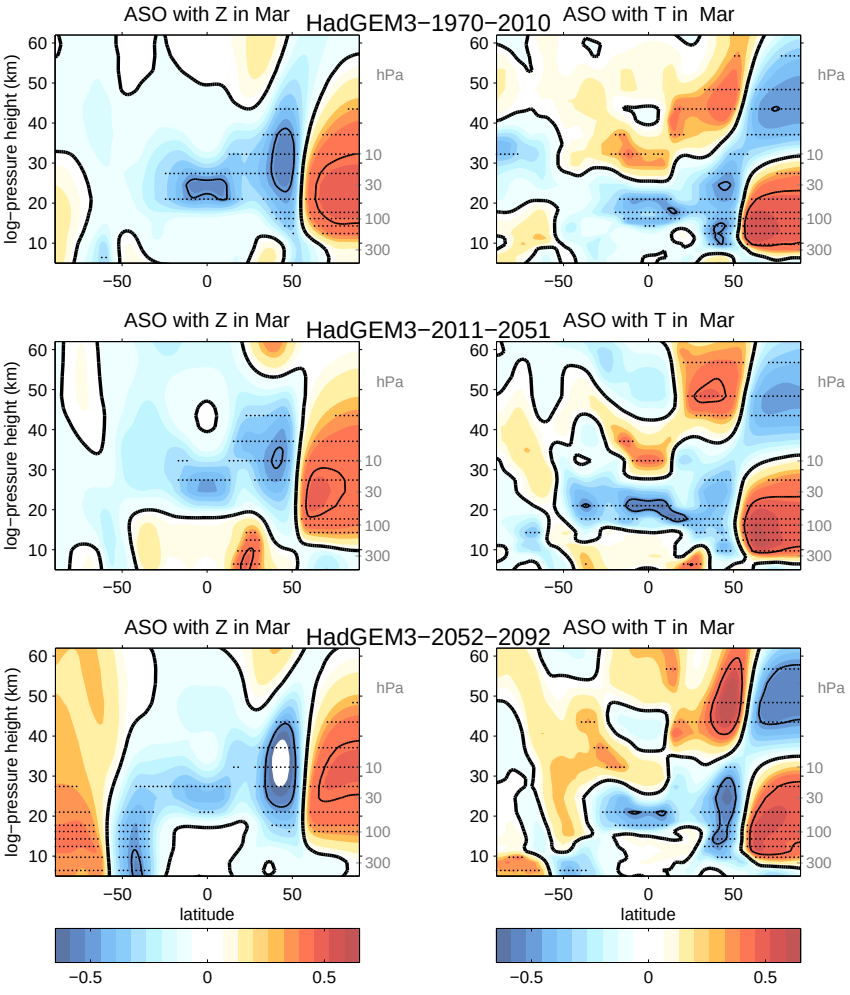

Fig. S 12. As in figure 2 of main body, but for HadGEM

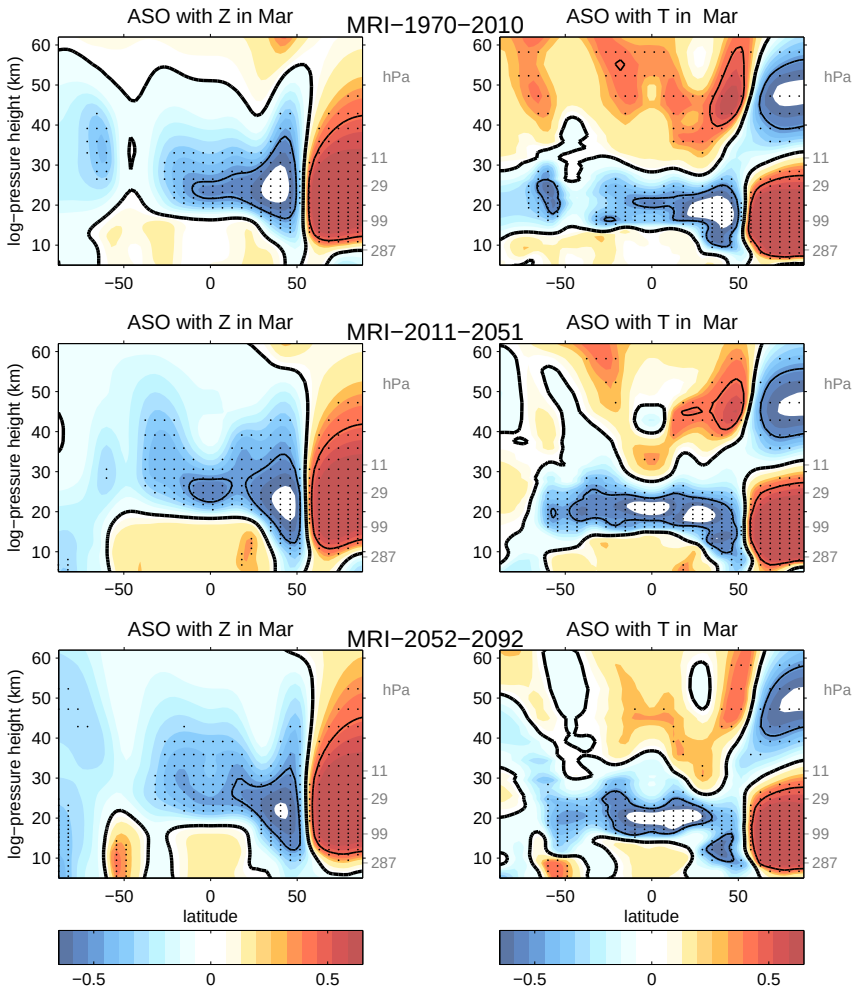

Fig. S 13. As in figure 2 of main body, but for MRI

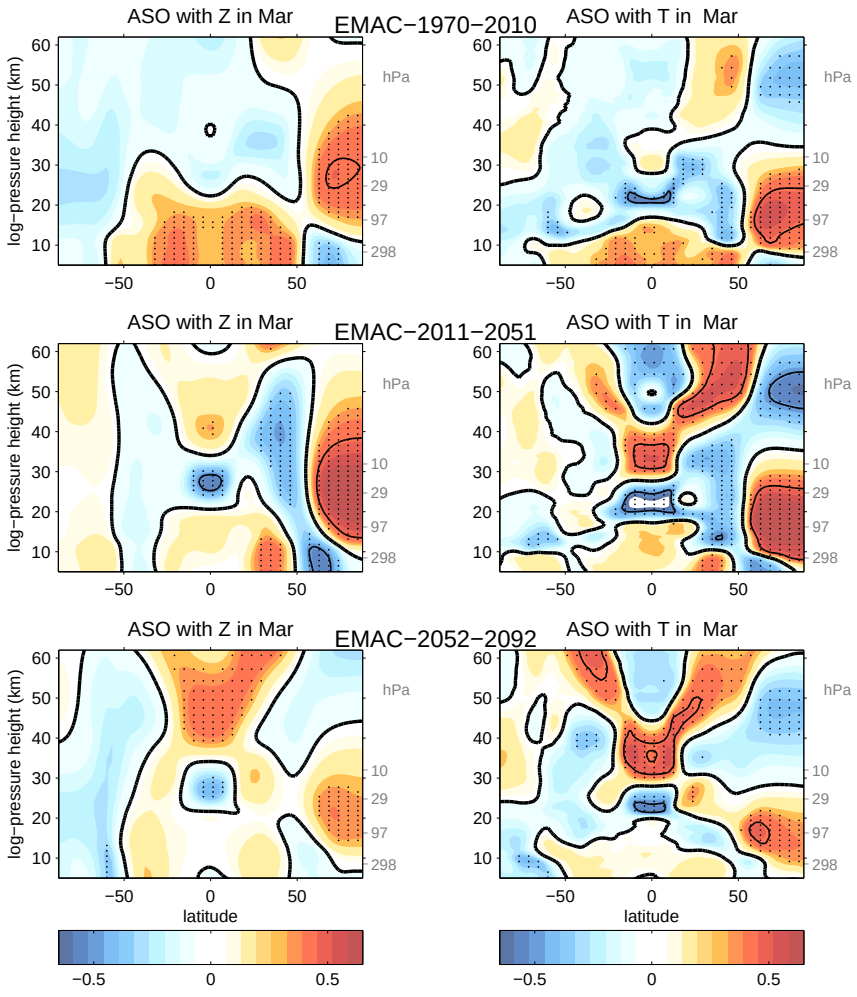

Fig. S 14. As in figure 2 of main body, but for EMAC

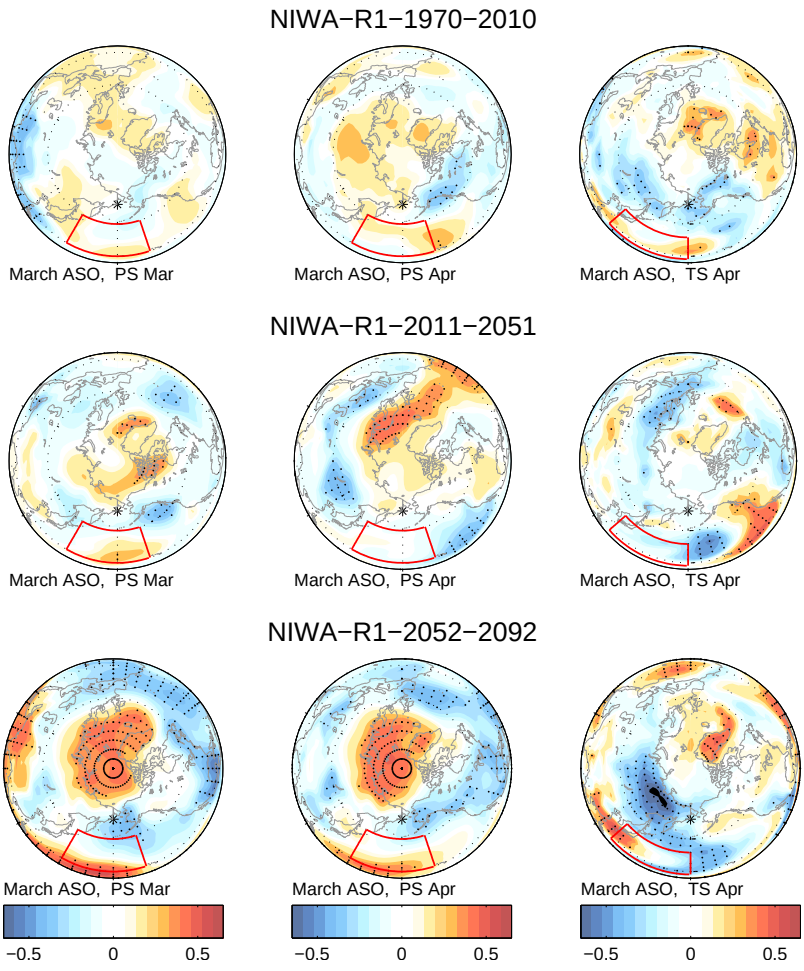

Fig. S 15. As in figure 5 of main body, but for Niwa run #1

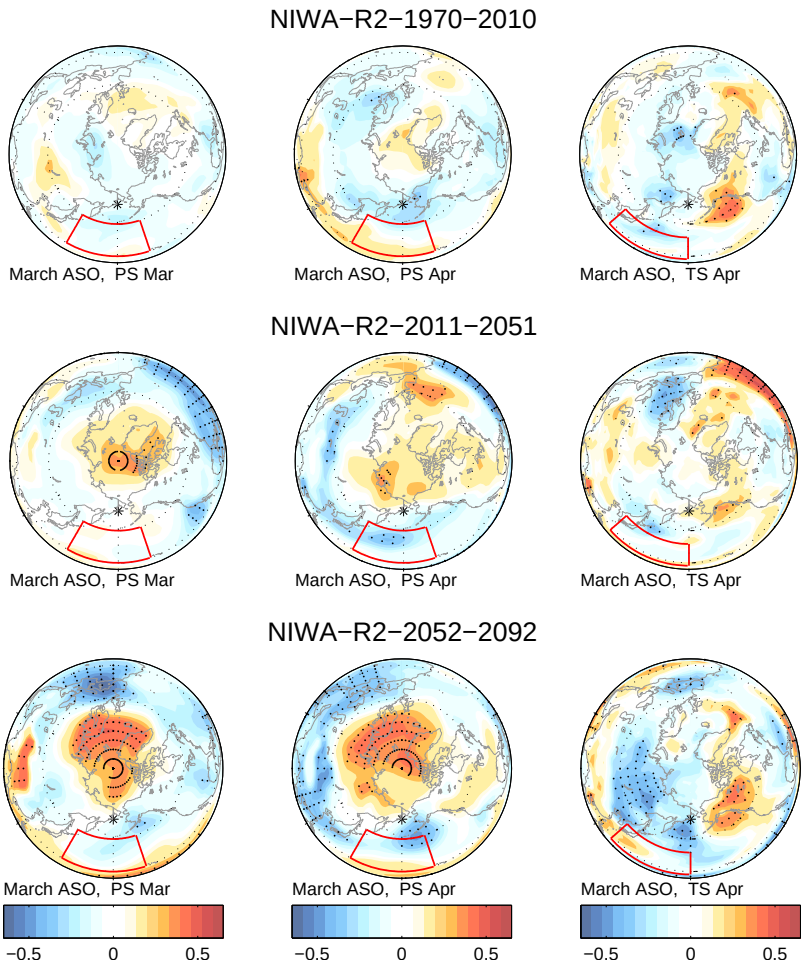

Fig. S 16. As in figure 5 of main body, but for Niwa run #2

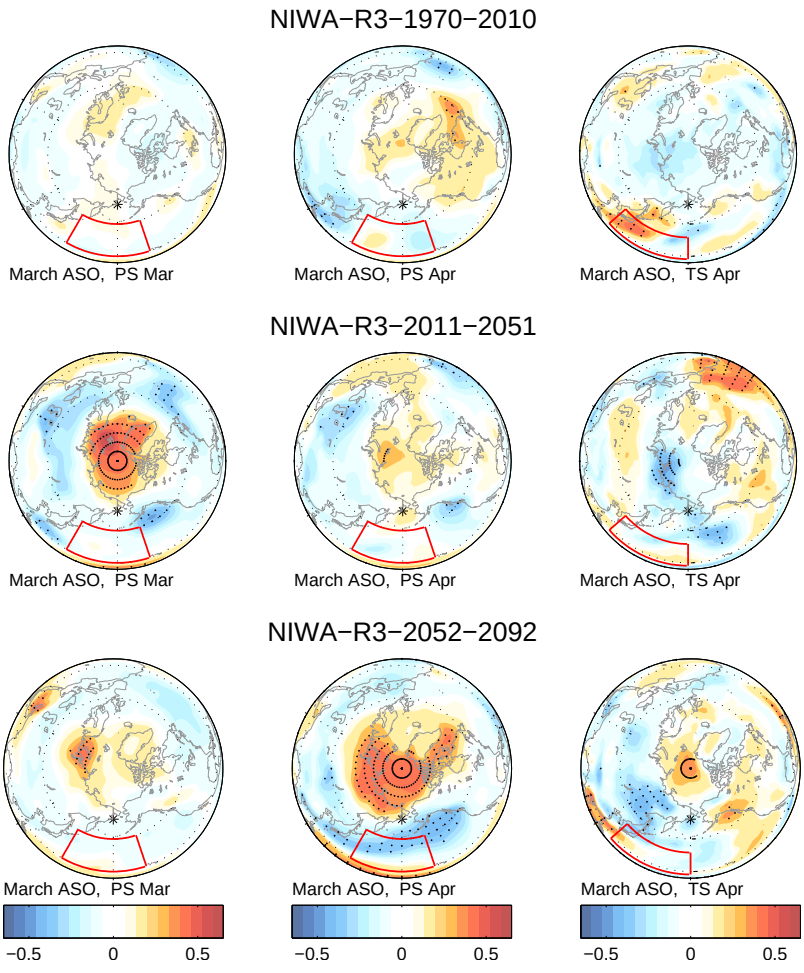

Fig. S 17. As in figure 5 of main body, but for Niwa run #3

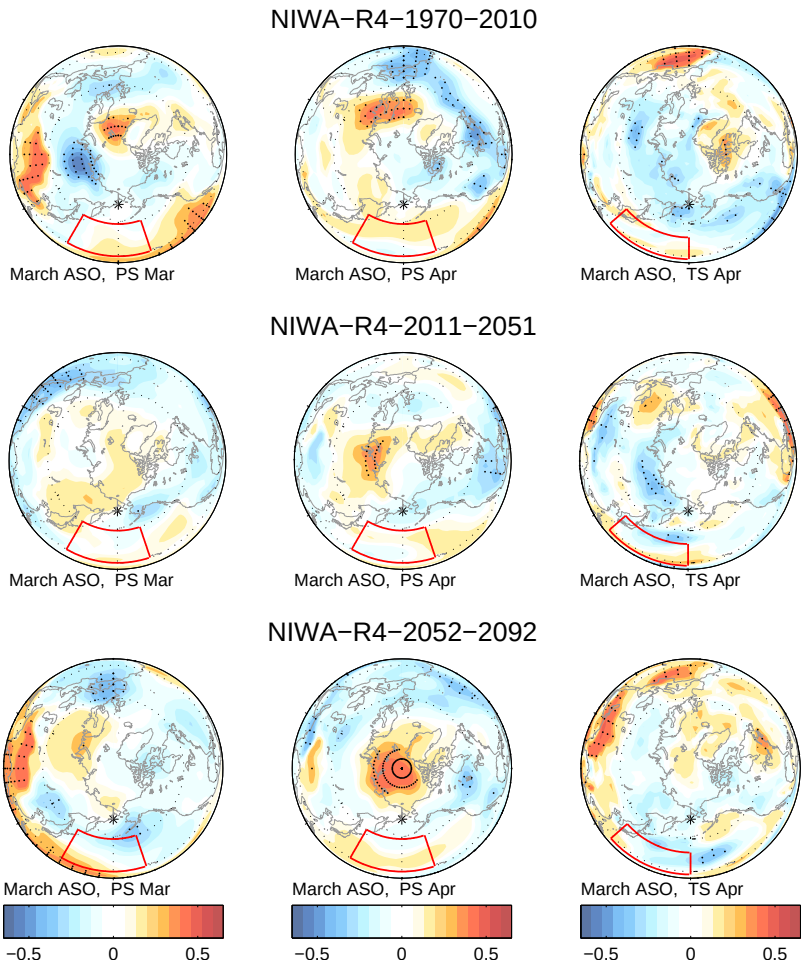

Fig. S 18. As in figure 5 of main body, but for Niwa run #4

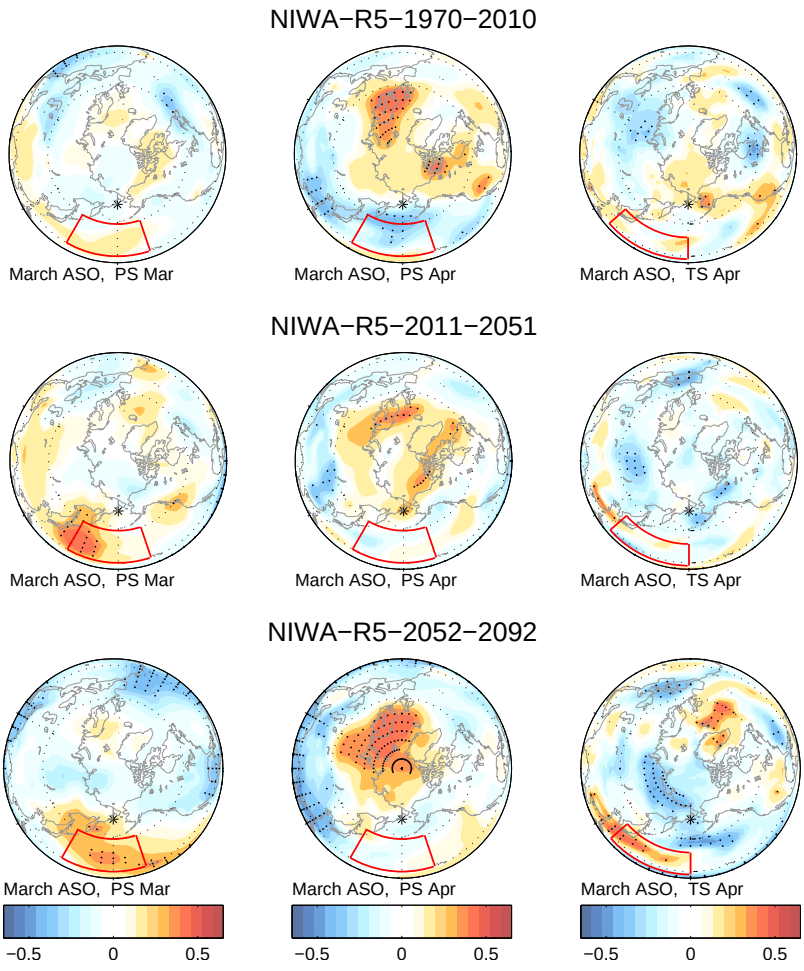

Fig. S 19. As in figure 5 of main body, but for Niwa run #5

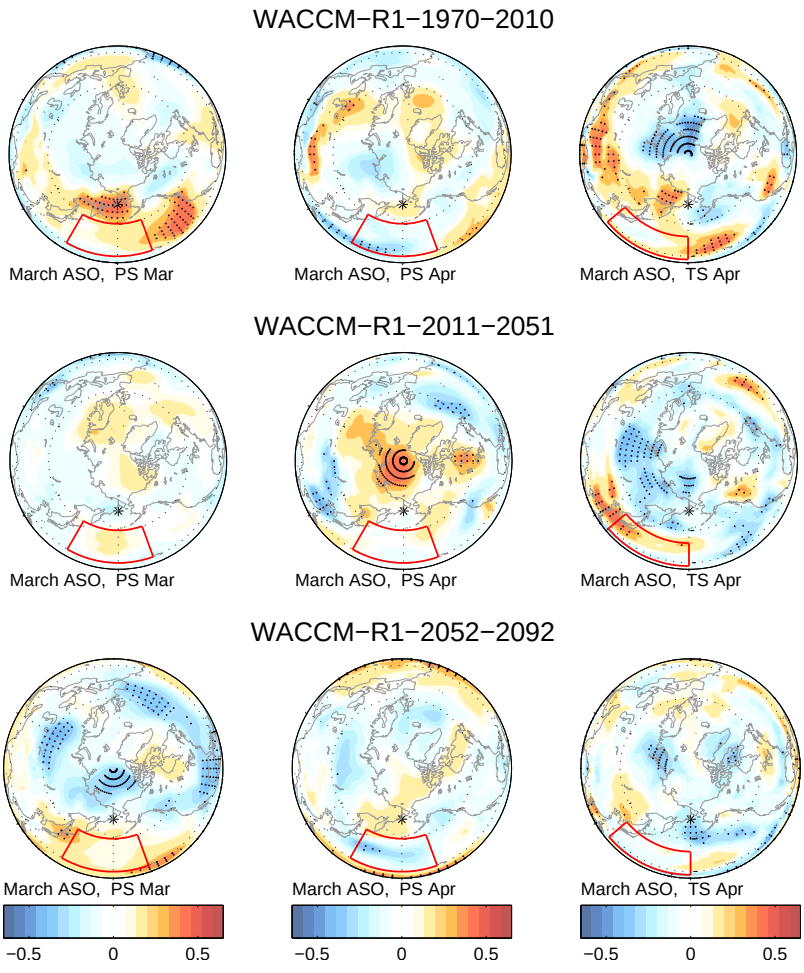

Fig. S 20. As in figure 5 of main body, but for NCAR-WACCM run #1

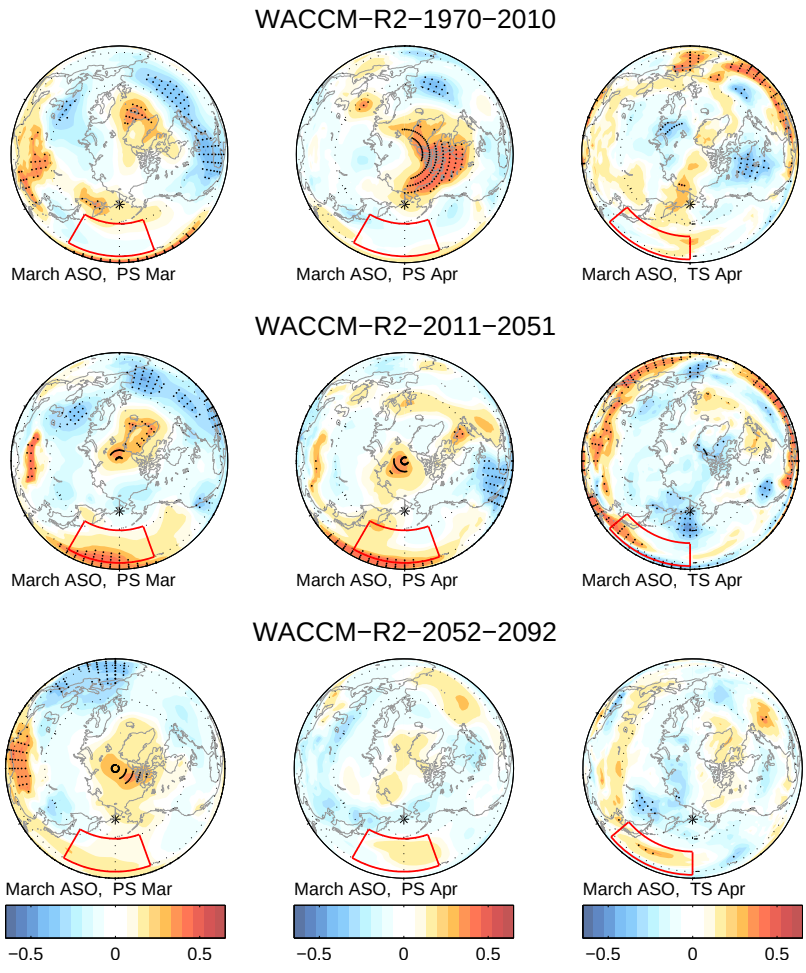

Fig. S 21. As in figure 5 of main body, but for NCAR-WACCM run #2

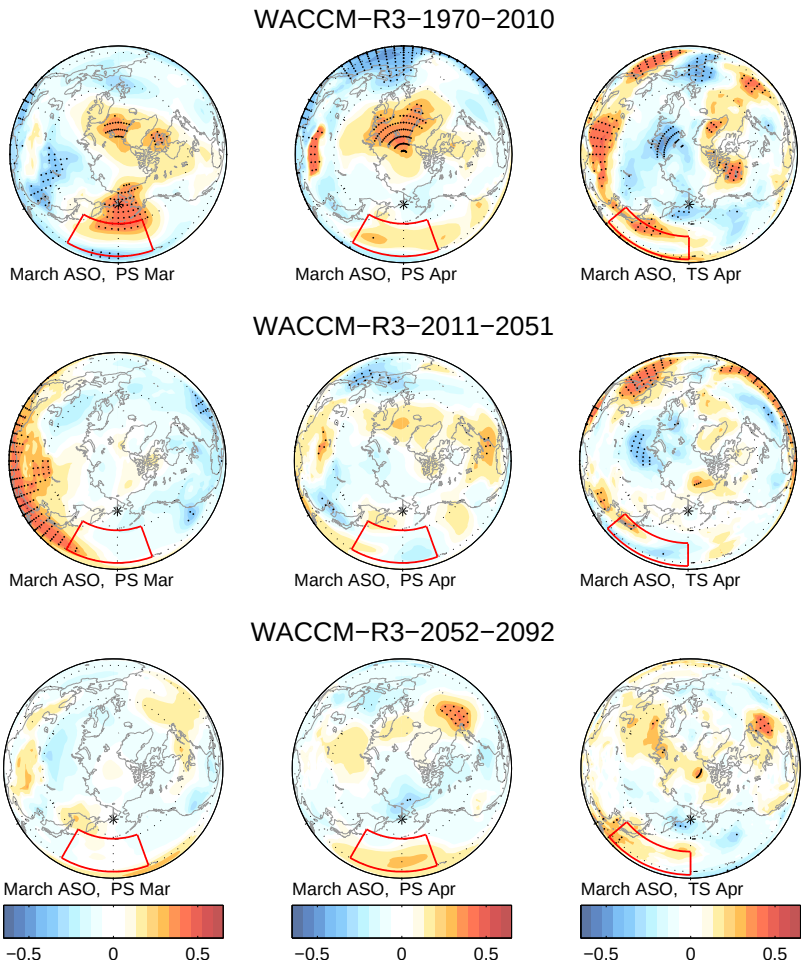

Fig. S 22. As in figure 5 of main body, but for NCAR-WACCM run #3

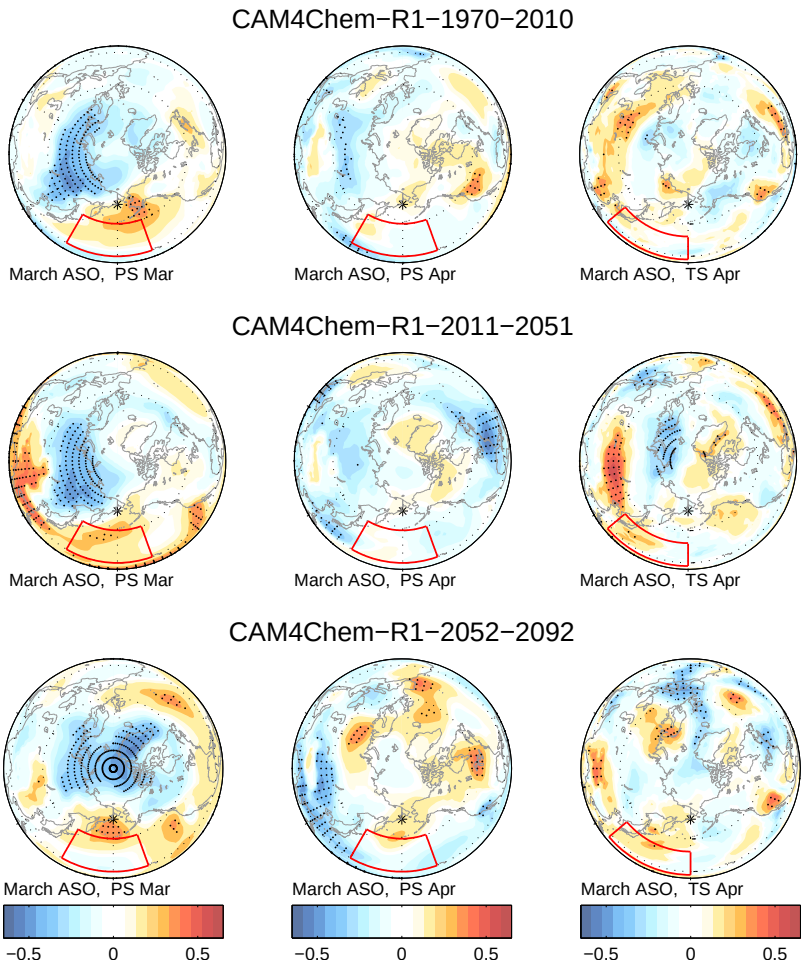

Fig. S 23. As in figure 5 of main body, but for NCAR-CAM4Chem run #1

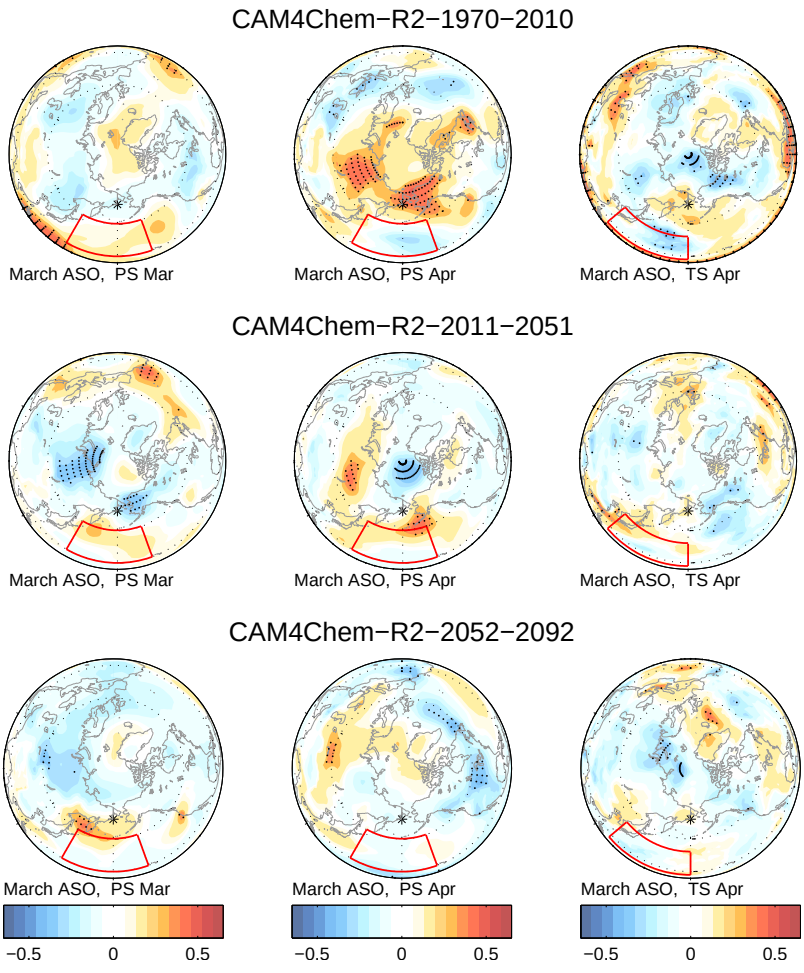

Fig. S 24. As in figure 5 of main body, but for NCAR-CAM4Chem run #2

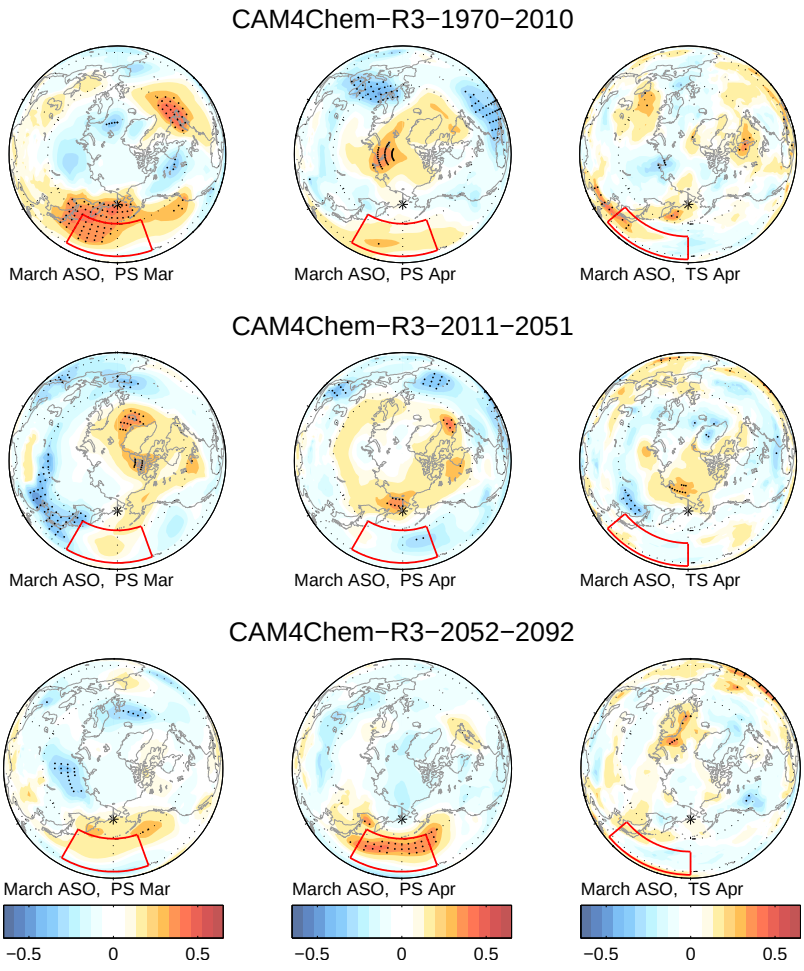

Fig. S 25. As in figure 5 of main body, but for NCAR-CAM4Chem run #3

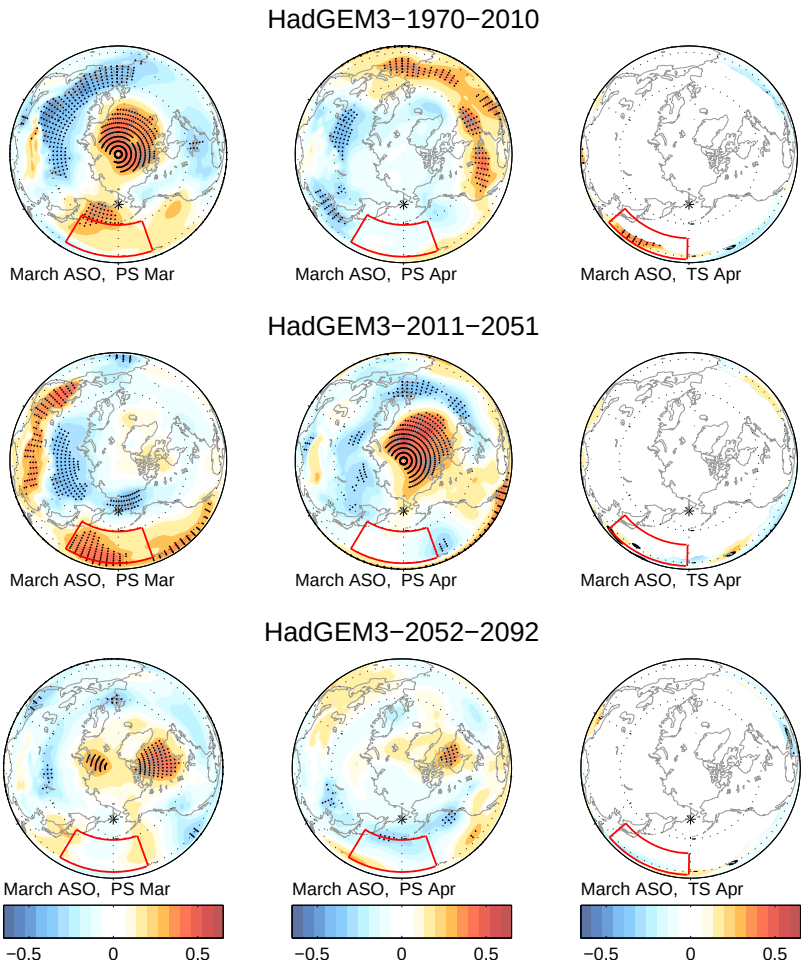

Fig. S 26. As in figure 5 of main body, but for HadGEM

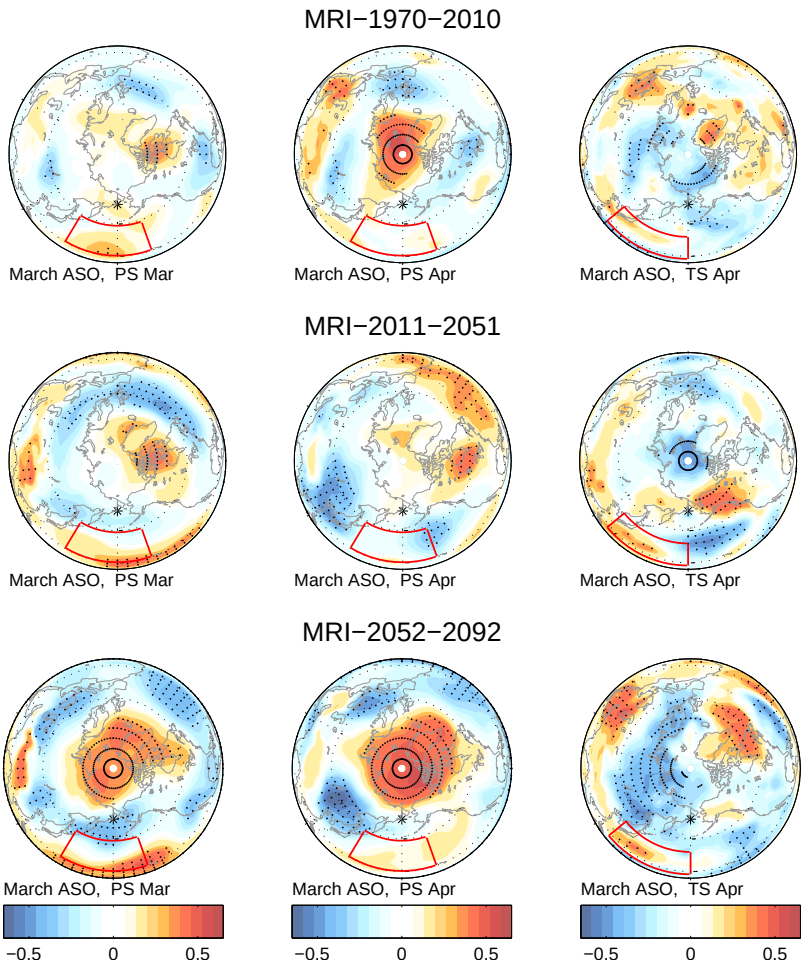

Fig. S 27. As in figure 5 of main body, but for MRI

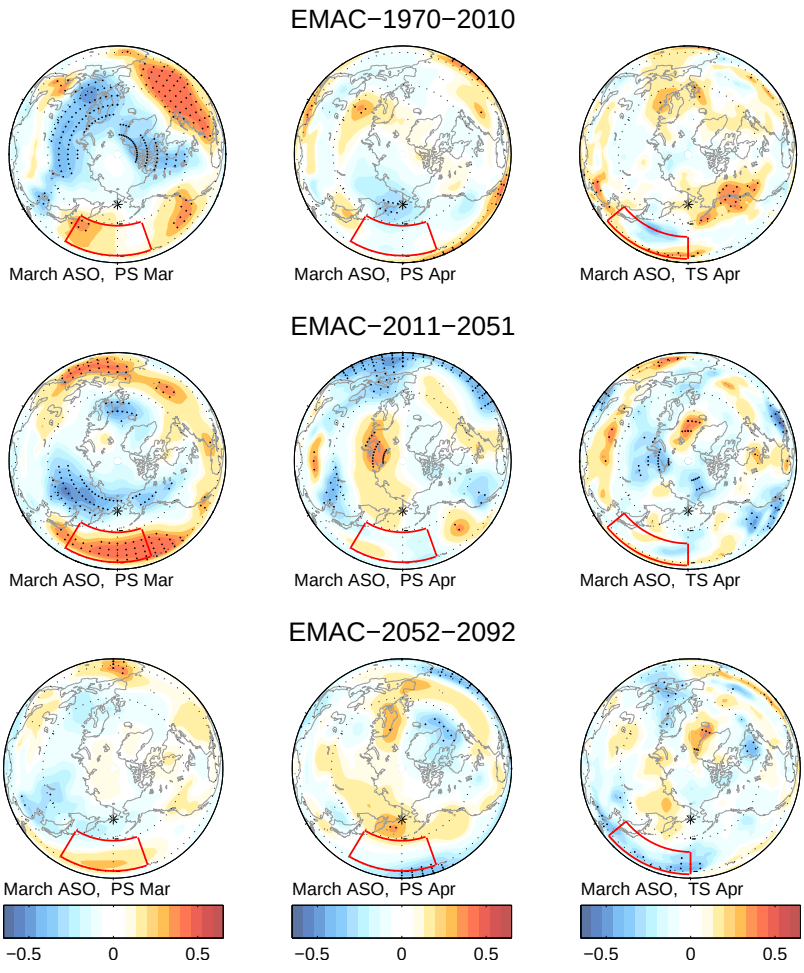

Fig. S 28. As in figure 5 of main body, but for EMAC

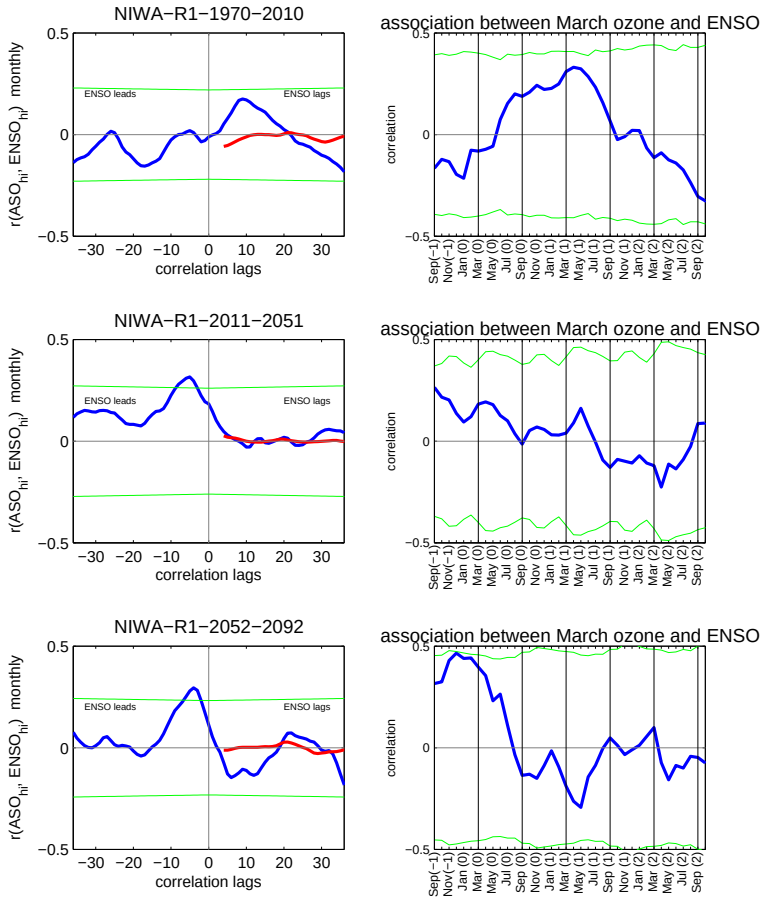

Fig. S 29. As in figure 6 of main body, but for Niwa run #1

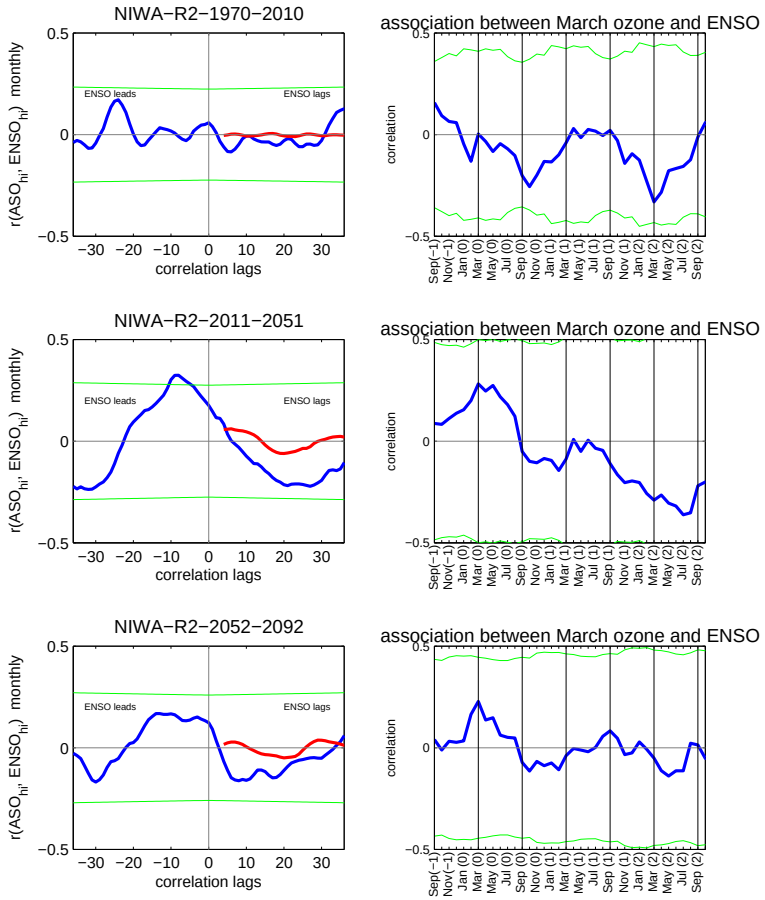

Fig. S 30. As in figure 6 of main body, but for Niwa run #2

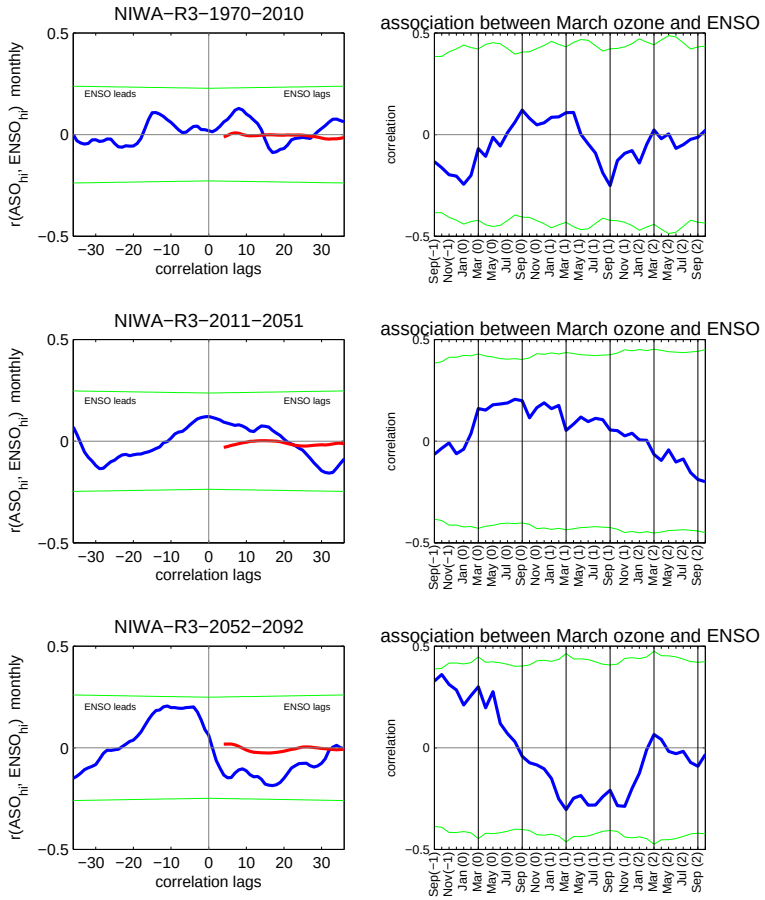

Fig. S 31. As in figure 6 of main body, but for Niwa run #3

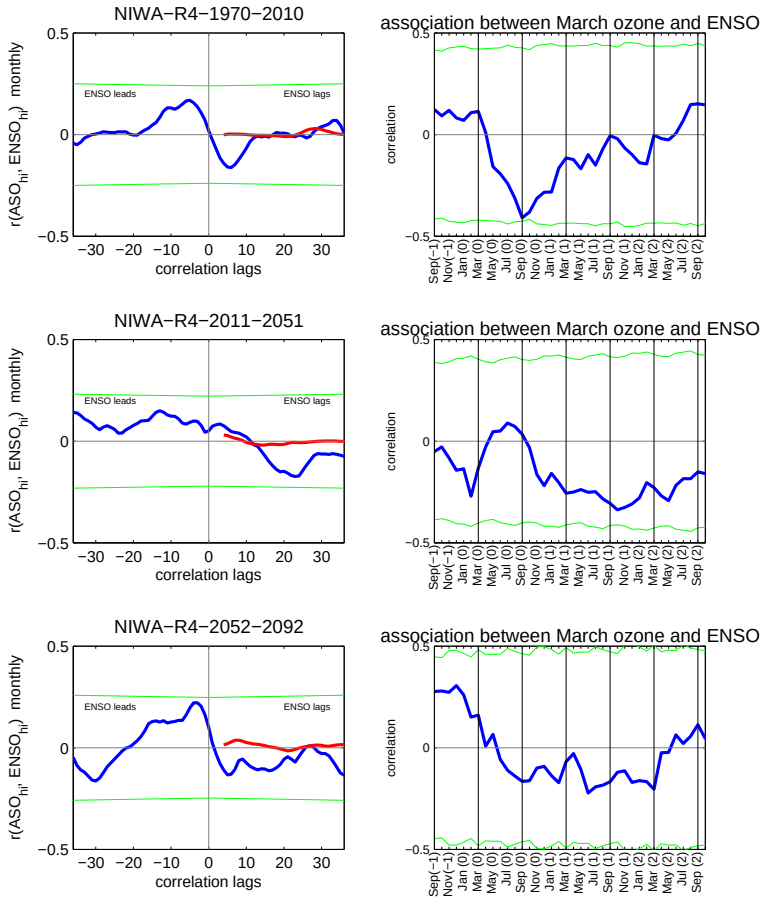

Fig. S 32. As in figure 6 of main body, but for Niwa run #4

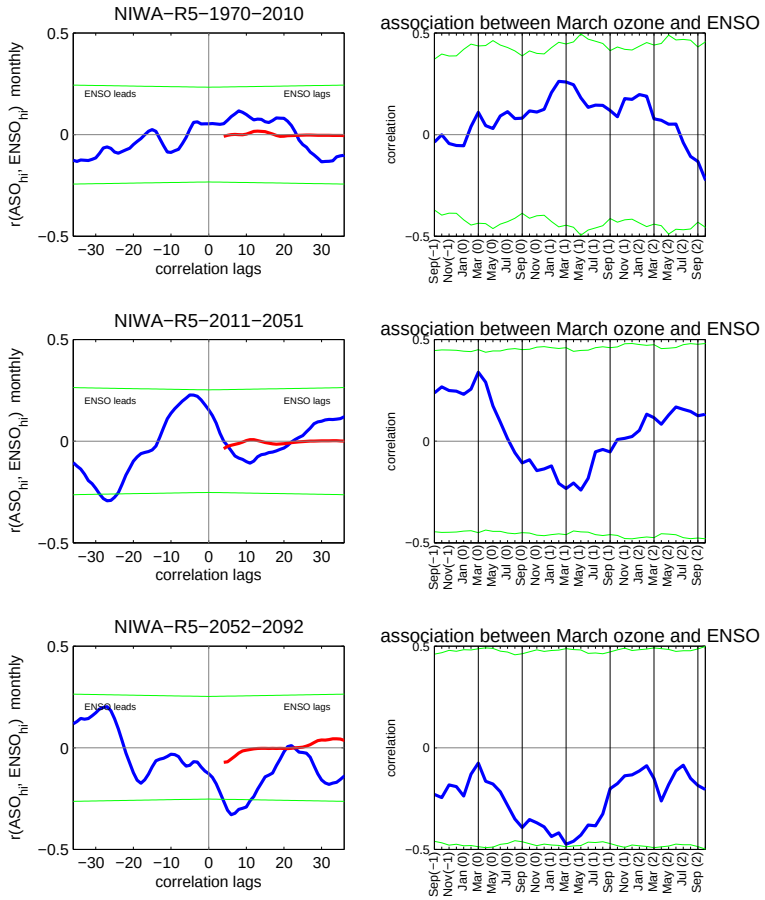

Fig. S 33. As in figure 6 of main body, but for Niwa run #5

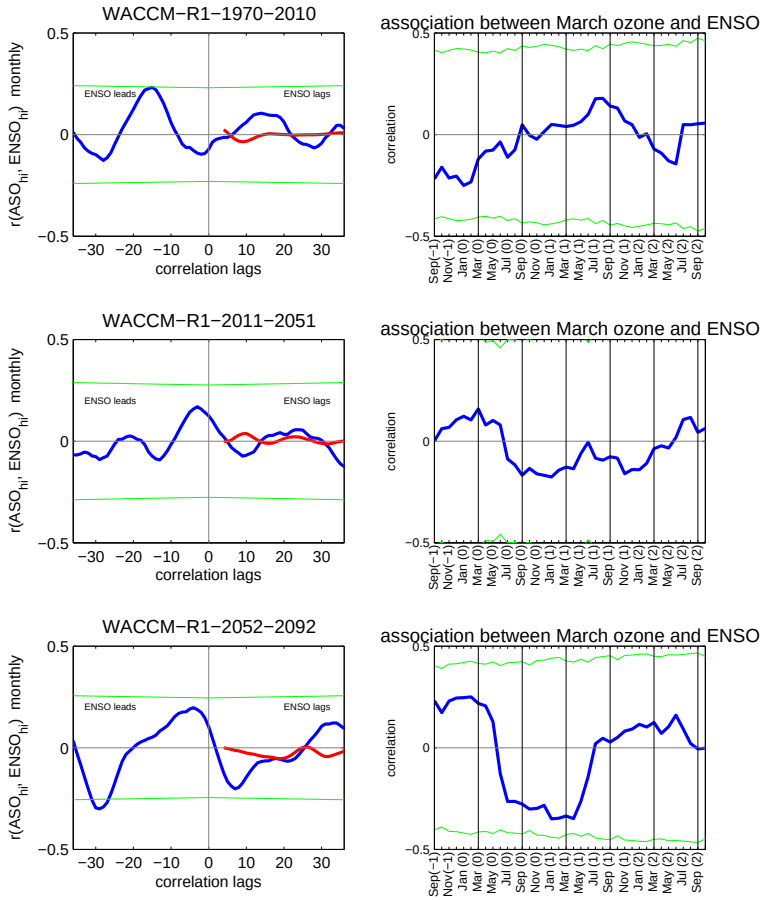

Fig. S 34. As in figure 6 of main body, but for NCAR-WACCM run #1

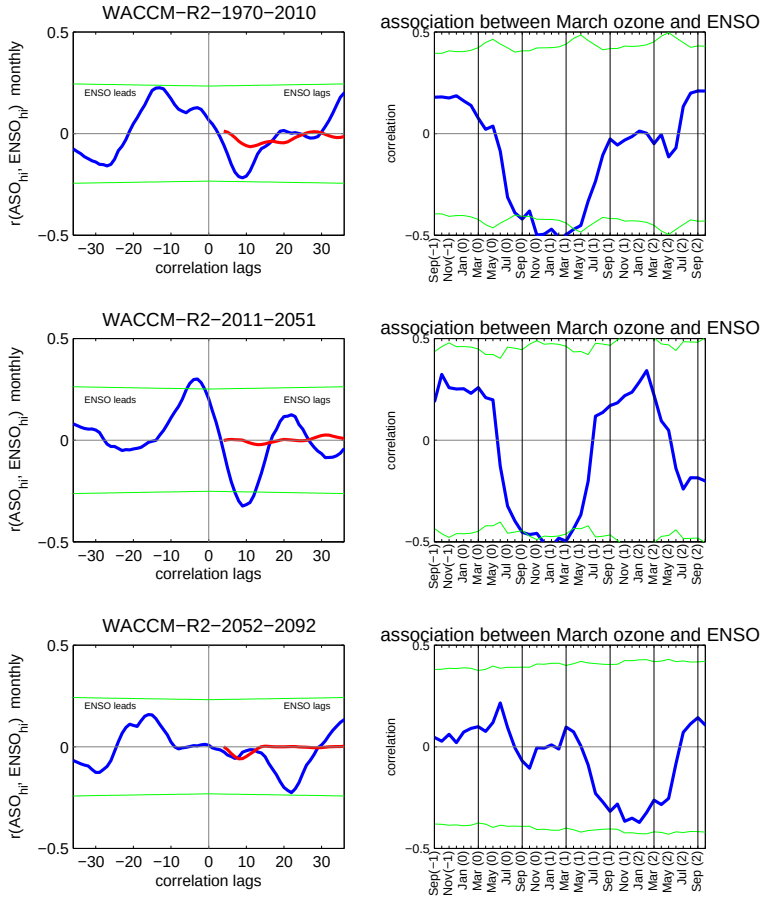

Fig. S 35. As in figure 6 of main body, but for NCAR-WACCM run #2

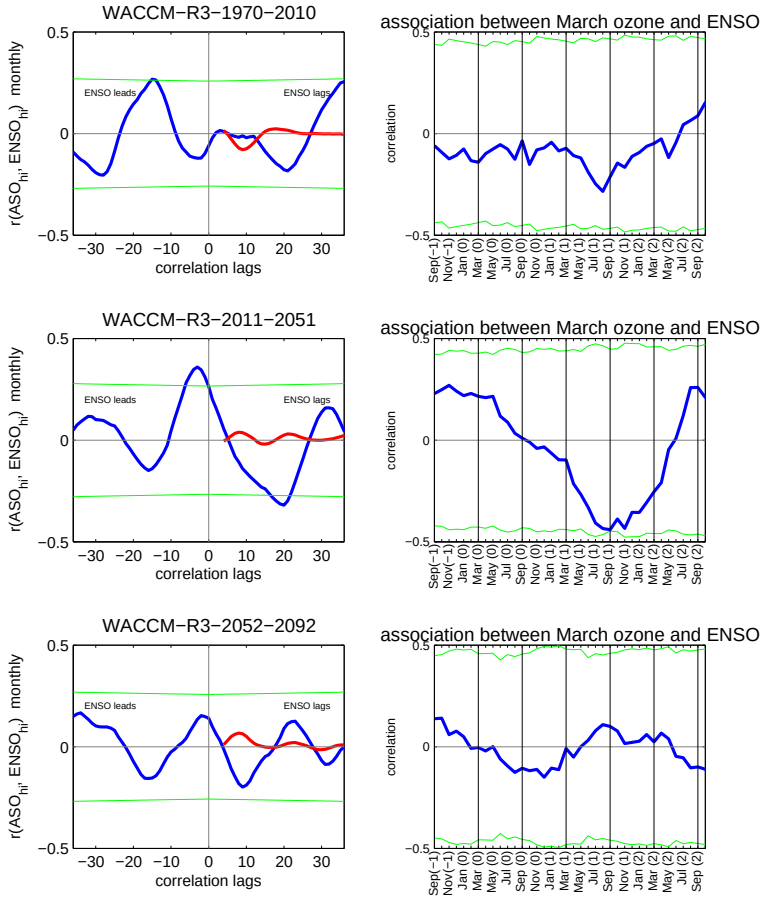

Fig. S 36. As in figure 6 of main body, but for NCAR-WACCM run #3

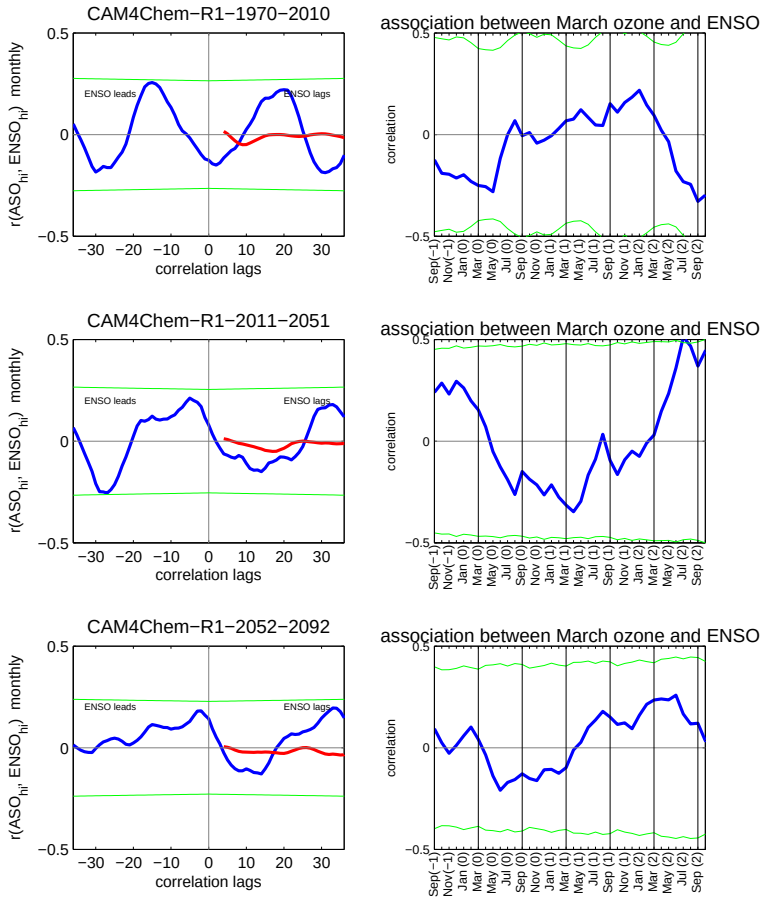

Fig. S 37. As in figure 6 of main body, but for NCAR-CAM4Chem run #1

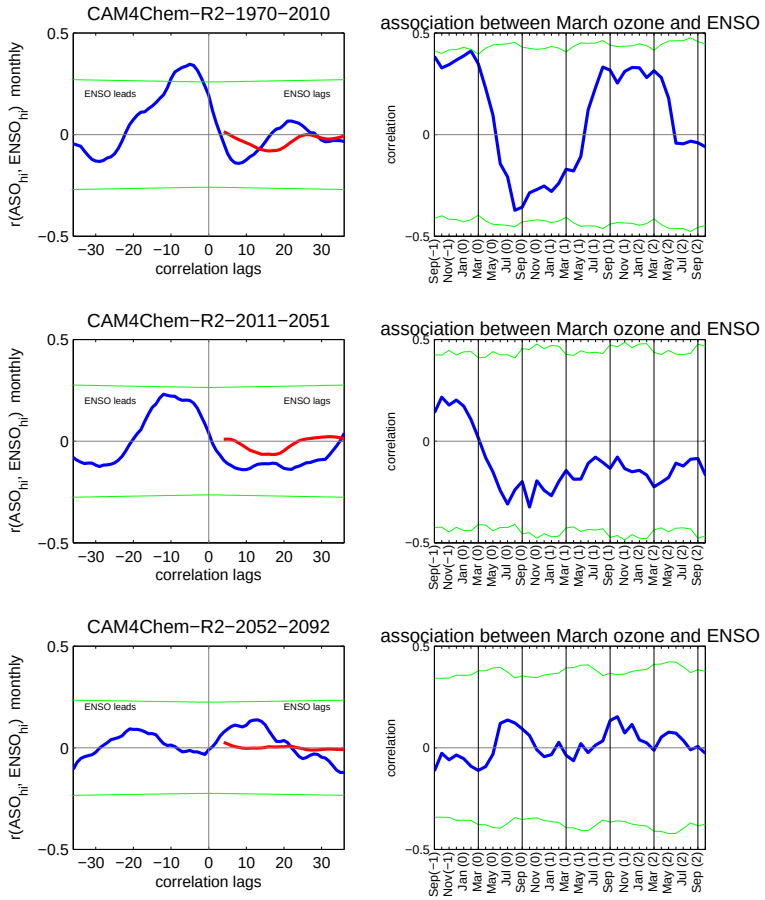

Fig. S 38. As in figure 6 of main body, but for NCAR-CAM4Chem run #2

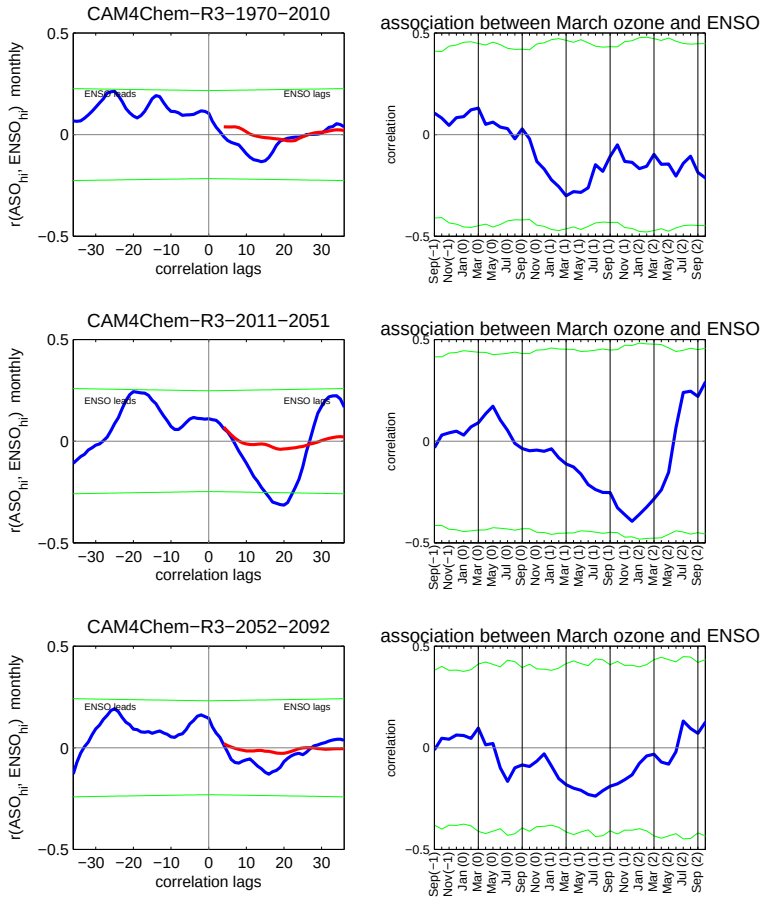

Fig. S 39. As in figure 6 of main body, but for NCAR-CAM4Chem run #3

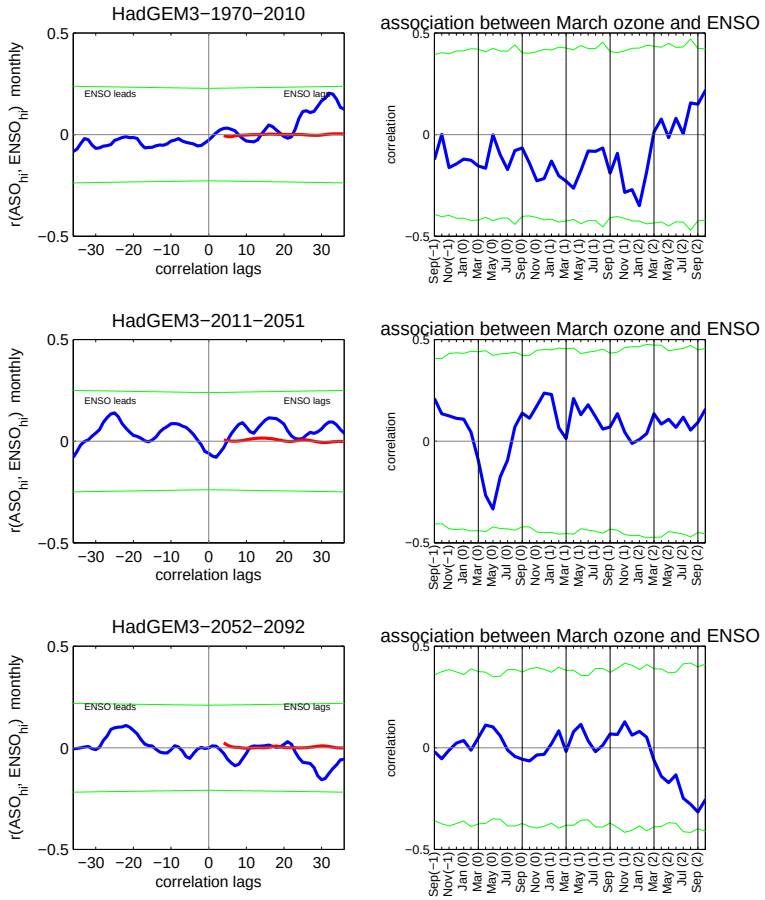

Fig. S 40. As in figure 6 of main body, but for HadGEM

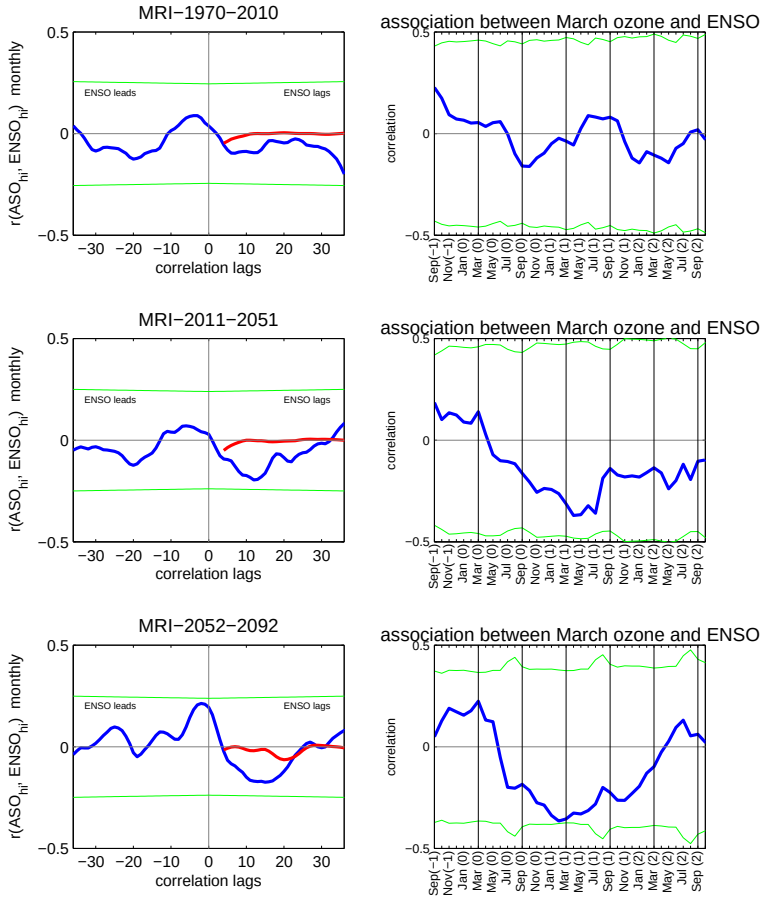

Fig. S 41. As in figure 6 of main body, but for MRI

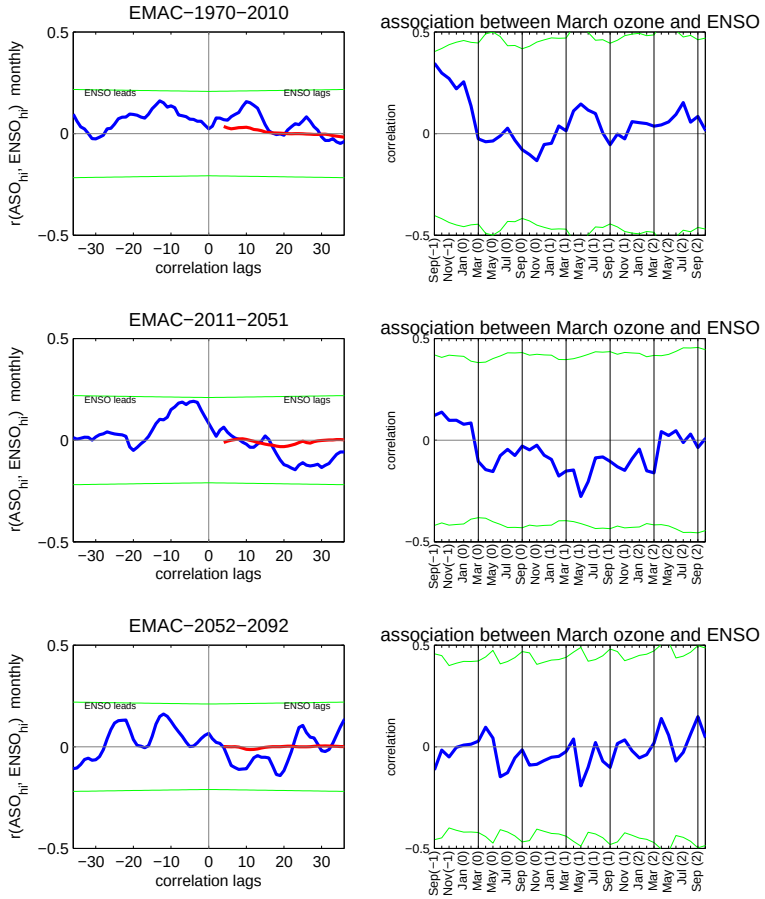

Fig. S 42. As in figure 6 of main body, but for EMAC

Acknowledgements. CIG was supported by the Israel Science Foundation (grant number 1558/14) and by a European Research Council starting grant under the European Union's Horizon 2020 research and innovation programme (grant agreement No 677756). We thank those involved in model development at GSFC-GMAO, and support by the NASA MAP program. We thank Valentina Aquila for performing some of the experiments discussed here, and Darryn W Waugh and Margaret M Hurwitz for suggestions. High-performance computing resources were provided by the NASA Center for Climate Simulation (NCCS). Correspondence and requests for data should be addressed to C.I.G. (email: chaim.garfinkel@mail.huji.ac.il). El Niño indices based on the ERSSTv4 data were downloaded from cpc.ncep.noaa.gov/data/indices/ersst4.nino.mth.81-10.ascii.

References